Draft version June 9, 2026
Typeset using LaTeX **twocolumn** style in AASTeX7.0.1

Spatially Resolving a Fiducial Thermal Nebula Driven by Draco C1, an Extragalactic Symbiotic Star

J. M. Wrobel,[1] T. J. Maccarone,[2] and J. D. Linford[1]

[1] *National Radio Astronomy Observatory, P.O. Box O, Socorro, NM 87801, USA*
[2] *Department of Physics and Astronomy, Texas Tech University, Box 41051, Lubbock, TX 79409-1051, USA*

(Received as ngVLA Memo # 139)

ABSTRACT

Symbiotic stars (SySts) are detached, interacting binary systems with a hot compact star, usually a white dwarf, accreting from the wind of a late-type giant star. Some SySts are known to be surrounded by thermal radio nebulae. Spatially resolved images of the nebulae encode information about how their formation and evolution are driven by the SySts. Draco C1 is a SySt in the Draco dwarf spheroidal galaxy at a distance of 82 kpc. Here, we explore whether the ngVLA could spatially resolve the continuum emission from a fiducial thermal nebula surrounding Draco C1. We find that this is doable with an on-target time of 38 h in Band 2, using the full ngVLA tapered to achieve an angular resolution of 7 mas at FWHM and an RMS noise 0.022 μJy beam^{-1}. Discovery of a spatially resolved thermal nebula surrounding Draco C1 could be followed up to infer physical parameters of the nebula (e.g., electron density, mass) and of the SySt (e.g., interaction zone between the stellar winds, orbital pole of the binary, rate of mass loss from the white dwarf).

Keywords: Draco dwarf galaxy (408); Symbiotic binary stars (1674); White dwarf stars (1799); Late-type giant stars(908)

1. CONTEXT & MOTIVATION

Symbiotic stars (SySts) are detached, interacting binary systems with a hot compact star, usually a white dwarf (WD), that accretes from the wind from a late-type giant star. Photometric and spectroscopic studies in the time domain show that some SySt traits exhibit periodic modulation. The binary orbital periods range from years for the S-type systems featuring a normal giant, to decades for the D-type systems featuring a dusty Mira variable. Given the periods and stellar masses involved, the binary orbits have separations of less than or about 100 au and cannot be spatially resolved, even at Galactic distances. These aforementioned topics are reviewed by Merc (2025).

Confirmed SySts appear to be rare (Merc et al. 2019), with Galactic and extragalactic counts of only 284 and 71 as of 2024[3]. However, from a combination of empirical and binary synthesis models, Laversveiler et al. (2025) estimate 1-50 thousand SySts within a Galactic radius of 10 kpc. This suggests that much of the SySt population in the Galaxy awaits discovery and subsequent characterization. Machine learning is also starting to help sharpen estimates of the full Galactic population (e.g., Akras et al. 2021; Contreras Rojas et al. 2026). Merc et al. (2019) also catalog 107 candidate SySts in galaxies as distant as the Virgo Cluster, presaging the potential growth of confirmed extragalactic SySts.

Most confirmed SySts, 247 of 284, are thought to be powered by stable nuclear hydrogen burning on the surface of the WD (Merc et al. 2019, and references therein). This scenario is physically possible for only a certain range of accretion rates onto the WD (Tutukov & Yungel'son 1976; Paczynski & Zytkow 1978). During this stable, quiescent state, an intense source of radiation ionizes some portion of the giant star's wind, thus yielding a thermal nebula (e.g., Skopal et al. 2017). Constraints on the integrated properties of a thermal nebula can be obtained from spectroscopy of well-known optical emission lines (e.g., Kuuttila & Gilfanov 2021) or from continuum emission at radio (e.g., Seaquist et al. 1993; Dickey et al. 2021) and millimeter wavelengths (e.g., Ivison et al. 1995; Tandoi et al. 2026).

The strongest constraints are expected to come from the 19 confirmed SySts with spatially resolved nebulae, only one of which is extragalactic (Merc et al. 2019).

Corresponding author: J. M. Wrobel
Email: jwrobel@nrao.edu

[3] https://astronomy.science.upjs.sk/symbiotics/about.html

Such nebulae can provide key information about how their formation and evolution are driven by the SySts in their quiescent state (e.g., Corradi et al. 1999; Kenny & Taylor 2005; Kuuttila & Gilfanov 2021). Some traits may evolve on the timescales of the binaries' orbital periods, while other traits may evolve secularly over longer timescales (e.g., Kenny & Taylor 2007; Skopal & Cariková 2015). In addition, spatially resolved thermal nebula can show substructure that may be linked to changes in the mass-loss rate from the WD (e.g., Kenny & Taylor 2007).

Here, we study the prospects for using the Next Generation Very Large Array (ngVLA; Selina et al. 2018) to spatially resolve a fiducial thermal nebula driven by Draco C1, a SySt in the Draco dwarf spheroidal galaxy at a distance $D = 82 \pm 2$ kpc (Kinemuchi et al. 2008). If this can be done for Draco C1, it clearly bodes well for being feasible for similar radio nebulae among the full Galactic population of 1-50 thousand SySts, as estimated by Laversveiler et al. (2025).

Section 2 describes Draco C1's integrated properties based on literature data and new data from the NSF Jansky Very Large Array (JVLA; Perley et al. 2011). Section 3 describes the integrated properties of the fiducial nebula if placed at the distance of Draco C1, and investigates the possibility of spatially resolving the fiducial nebula through ngVLA observations. A summary and conclusions appear in Section 4.

2. DRACO C1

At Draco's distance $D = 82 \pm 2$ kpc (Kinemuchi et al. 2008), 82 au subtend 1 mas.

2.1. *Integrated Non-Radio Properties*

Lewis et al. (2020, and references therein) used available photometric data and new near-infrared spectroscopic data on Draco C1 to improve the parameters for its cool, red giant (RG) component; to constrain the temperature and mass of its hot, WD companion; and to constrain the orbital parameters for the RG-WD binary. (Lewis et al. (2020) did not specify which spectroscopic features they examined, but a similar study from the same team (Washington et al. 2021) used Brackett and metal absorption lines.) Importantly, Lewis et al. (2020) inferred a precise orbital period $P = 3.3402^{+0.0096}_{-0.0101}$ yr and a minimum orbital separation $a_{\rm min} = 2.227^{+0.071}_{-0.069}$ au, which subtends 0.027 mas. The combination of stellar and orbital properties indicate that the WD is experiencing wind Roche lobe overflow, wherein the dense stellar wind from the RG, rather than the star itself, fills the Roche lobe.

2.2. *Integrated Radio Properties*

2.2.1. *Literature Data*

Literature radio data on Draco C1 are reported in Table 1. The observations' UT dates and array configurations were verified via the NRAO Data Archive[4]. The radio searches were conducted at the a priori positions, with subarcsecond accuracy, of optical or XMM-Newton counterparts to Draco C1 (Seaquist & Taylor 1990; Saeedi et al. 2019).

2.2.2. *New Data*

JVLA visibility data centered at a frequency $\nu = 1.5$ GHz were retrieved from the NRAO Data Archive (project code 24A-216, PI C. Kawai). Multiple observations were available and the one minimally affected by radio frequency interference was selected. Table 1 gives some observation details. A coordinate equinox of 2000 was employed.

The pointing center was the nucleus of the Draco dwarf spheroidal galaxy, at a right ascension of 17h20m12.3874s and a declination of 57°54′55.1900″. The primary beam easily encompassed Draco C1, which is offset from the nucleus by about 5′ (120 pc). J1634+6245, at a right ascension of 16h34m33.803s and a declination of 62°45′35.903″, and with a 1D position error of 150 mas, was used as a complex gain calibrator. The switching time between it and the nucleus was 15 m.

Data were acquired in dual circular polarizations, each spanning 16×1 MHz of bandwidth. 3C 147 was observed to set the amplitude scale to an estimated accuracy of 5% (Perley & Butler 2017). The exposure time on Draco C1 was 94 m. Polarization calibration was not implemented as the observation spanned only 2 h. The visibility data were pipeline calibrated and imaged using versions 6.6.6 and 6.6.6-17, respectively, of the Common Astronomy Software Applications (CASA; CASA Team et al. 2022). Figure 1 shows the resulting primary-beam-corrected image near Draco C1.

The literature (Seaquist et al. 1984, 1993; Lacy et al. 2020) and new data impose 3σ upper limits on Draco C1's integrated luminosity density $L_\nu^{\rm Draco\,C1}$ at frequencies $\nu = 1.5-8.5$ GHz (Table 1, Figure 2). Given the tabulated θ_ν values, these upper limits are not compromised by emission from the unrelated source west of Draco C1 (Figure 1).

[4] https://data.nrao.edu

Table 1. Radio Photometry of Draco C1

UT Date	Frequency ν (GHz)	Configuration	FWHM Resolution θ_ν ($''$,$''$,$^\circ$)	Flux Density $S_\nu^{3\sigma}$ (μJy)	Luminosity Density L_ν (erg s^{-1} Hz^{-1})	Reference
(1)	(2)	(3)	(4)	(5)	(6)	(7)
2024 Jul 16	1.5	JVLA B	4.53, 3.80, −76.2	< 29	$< 2.3 \times 10^{20}$	1
2020 Aug 04	3.0	JVLA B	2.84, 2.35, −29.3	< 420	$< 3.4 \times 10^{21}$	2
1984 Nov 12	4.9	VLA A	0.48, 0.35, +62.0[a]	< 240	$< 1.9 \times 10^{21}$	3
1991 Feb 26	8.5	VLA D	13.64, 6.77, +57.6[a]	< 100	$< 8.0 \times 10^{20}$	4

[a] As estimated at https://www.vla.nrao.edu/astro/nvas/.

NOTE—References. (1) this work; (2) Lacy et al. (2020); (3) Seaquist & Taylor (1990); (4) Seaquist et al. (1993)

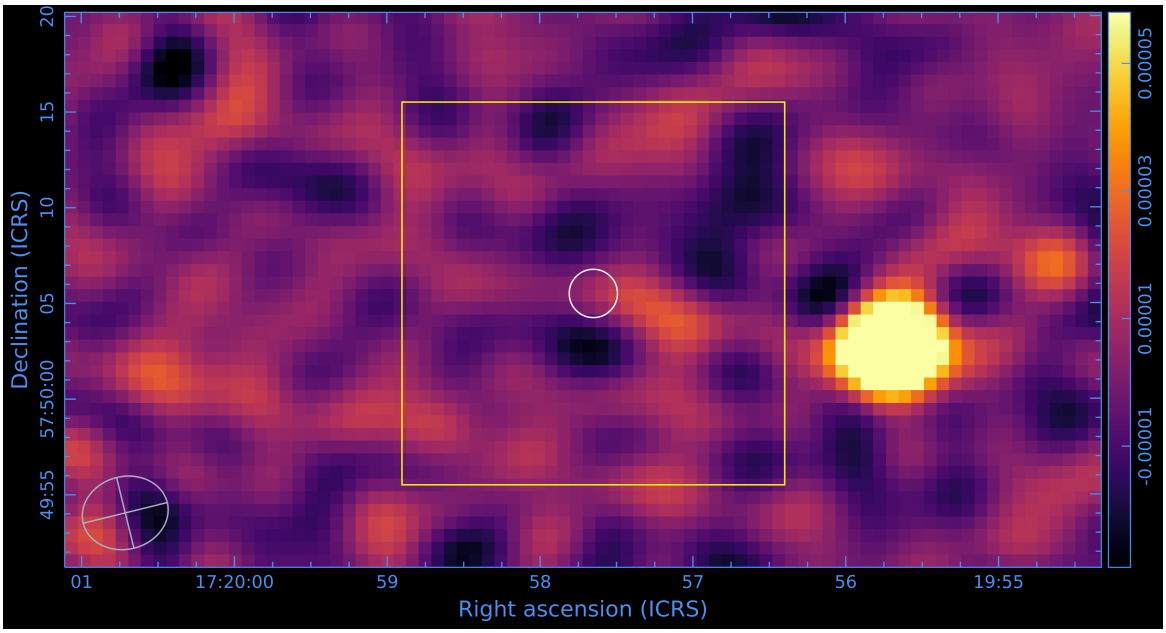

Figure 1. JVLA image of Stokes I emission at $\nu = 1.5$ GHz in the vicinity of Draco C1, visualized via The Cube Analysis and Rendering Tool for Astronomy (CARTA; Comrie et al. 2021). Grey ellipse shows $\theta_{1.5\,\mathrm{GHz}}$ at FWHM. Color bar linearly spans -30 to $+60\,\mu$Jy beam^{-1}. White circle conveys the 2D position uncertainty at 3σ of the XMM-Newton counterpart to Draco C1 (Saeedi et al. 2019). RMS noise is $\sigma = 9.7\,\mu$Jy beam^{-1} in the box of side $20''$ (8.0 pc) centered on the XMM-Newton position (Saeedi et al. 2019). The source with a peak of $170\,\mu$Jy beam^{-1} and to the west of the $20''$ search box has an infrared counterpart SSTSL2 J171955.68+575002.7[a] and is unrelated to Draco C1.

[a] https://ned.ipac.caltech.edu/

3. A FIDUCIAL THERMAL NEBULA

3.1. $D = 1.27$ *kpc (AG Peg)*

At AG Peg's Gaia distance $D = 1.27$ kpc (Bailer-Jones et al. 2021), 1270 au subtend $1''$.

Spatially extended emission from AG Peg was first reported by Ghigo & Cohen (1981), based on observations with the construction-era VLA at a frequency $\nu = 5$ GHz. VLA imaging with improved sensitivity and angular resolution soon identified the extended emission as arising from an inner shell-like nebula (Hjellming 1985; Kenny et al. 1991).

The integrated spectral index of the inner nebula at frequencies $\nu = 5-22$ GHz indicated optically thin thermal emission (Kenny et al. 1991; Ivison et al. 1995). Near a frequency $\nu = 8.5$ GHz, Dickey et al. (2021) reported an integrated spectral index $\alpha_{8.5\,\mathrm{GHz}} = -0.02 \pm 0.04$ ($S_\nu \propto \nu^\alpha$) and integrated optical depth $\tau_{8.5\,\mathrm{GHz}} =$

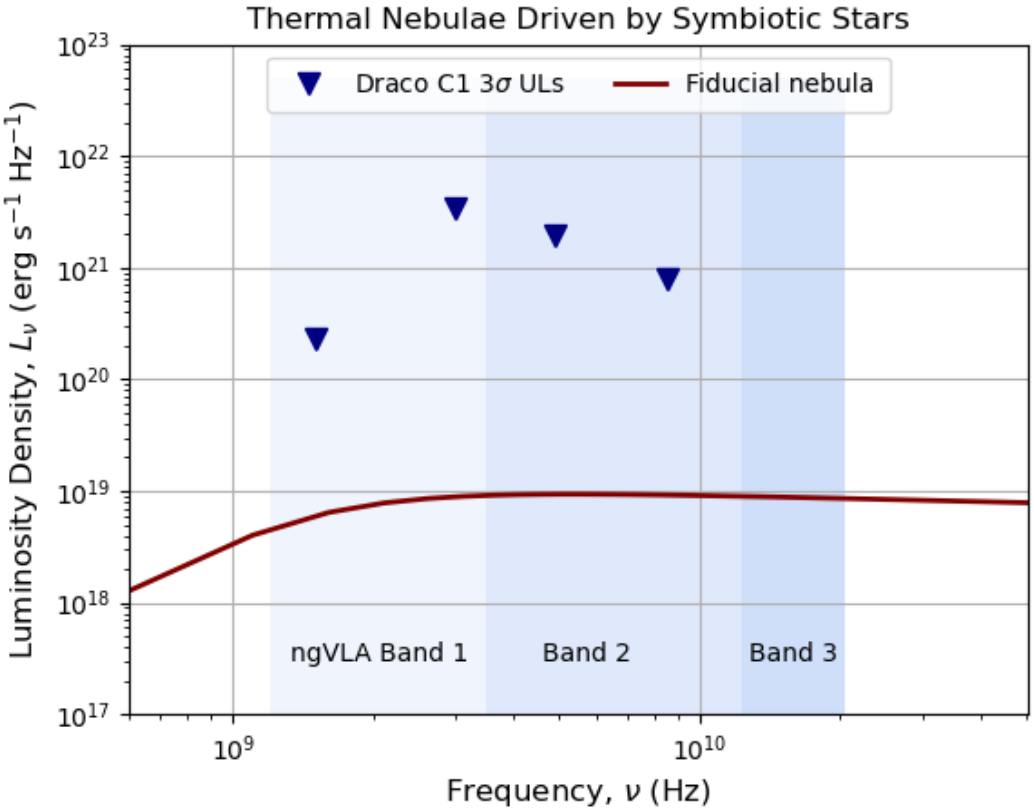

Figure 2. Comparing 3σ upper limits on Draco C1's integrated luminosity density $L_\nu^{\rm Draco\,C1}$ (Table 1) to the integrated luminosity density $L_\nu^{\rm fiducial}$ of a fiducial radio nebula (Section 3) placed at Draco C1's distance $D = 82 \pm 2$ kpc (Kinemuchi et al. 2008).

0.04 ± 0.02. This spectral model is anchored to the nebula's flux density $S_{8.5\,\rm GHz} = 6.6 \pm 0.1$ mJy (Ivison et al. 1995). Folding in the nebula's distance, the spectral model yields the integrated luminosity density $L_\nu^{\rm fiducial}$ shown in Figure 2. Also, for an assumed electron temperature of 10^4 K, Dickey et al. (2021) estimated an integrated brightness temperature of 400 ± 200 K near a frequency $\nu = 8.5$ GHz.

The spatially-resolved inner radio nebula of AG Peg is selected as a fiducial thermal nebula. Its best available images are from Kenny & Taylor (2007) at a frequency $\nu = 5$ GHz and are shown in Figure 3. The images span 1984 to 1991, when this S-type, shell-burning SySt was in quiescence, long after a nova-like outburst in around 1850 and well before a subsequent outburst in 2015 (Skopal et al. 2017). For perspective, the Dickey et al. (2021) study involved 16 shell-burning SySts, including AG Peg. Those authors found that the integrated luminosity densities for the 16 peaked at $L_{8.5\,\rm GHz} \sim 10^{20}\,{\rm erg\,s^{-1}\,Hz^{-1}}$, with AG Peg having the lowest value at $L_{8.5\,\rm GHz} = 1.3 \times 10^{19}\,{\rm erg\,s^{-1}\,Hz^{-1}}$. This suggests that the inner nebula of AG Peg could be considered as being a conservative choice for a fiducial radio nebula.

Fitting a spherical shell model to the images of Figure 3, Kenny & Taylor (2007) inferred the nebula's outer and inner angular diameters, angular expansion rate, electron density, and mass. For context, the outer angular diameter of the nebula in 1984, $\theta = 1\farcs87 \pm 0\farcs04$, corresponds to a linear diameter $d = 2370 \pm 50$ au. The SySt binary consists of a WD and RG, and has an orbital period $P \sim 2.2$ yr (Meinunger 1981).

A spherical shell model is only a first-order representation of AG Peg's inner nebula. Each image in Figure 3 encompasses $(\frac{\pi}{4} \times 1\farcs87^2)/(0.5665 \times 0\farcs45^2) = 24$ synthesized beam areas. This is enough to search for substructure or changes in the nebula from epoch to epoch. Kenny & Taylor (2007) investigated whether such traits could be related to how the nebula was formed and evolves. To explore this topic, they adopted the general framework of a colliding wind (CW) model (Seaquist et al. 1984; Nussbaumer & Vogel 1987; Kenny et al. 1991; Kenny & Taylor 2005) and enhanced it to consider how the binary's orbital traits could influence the nebula's

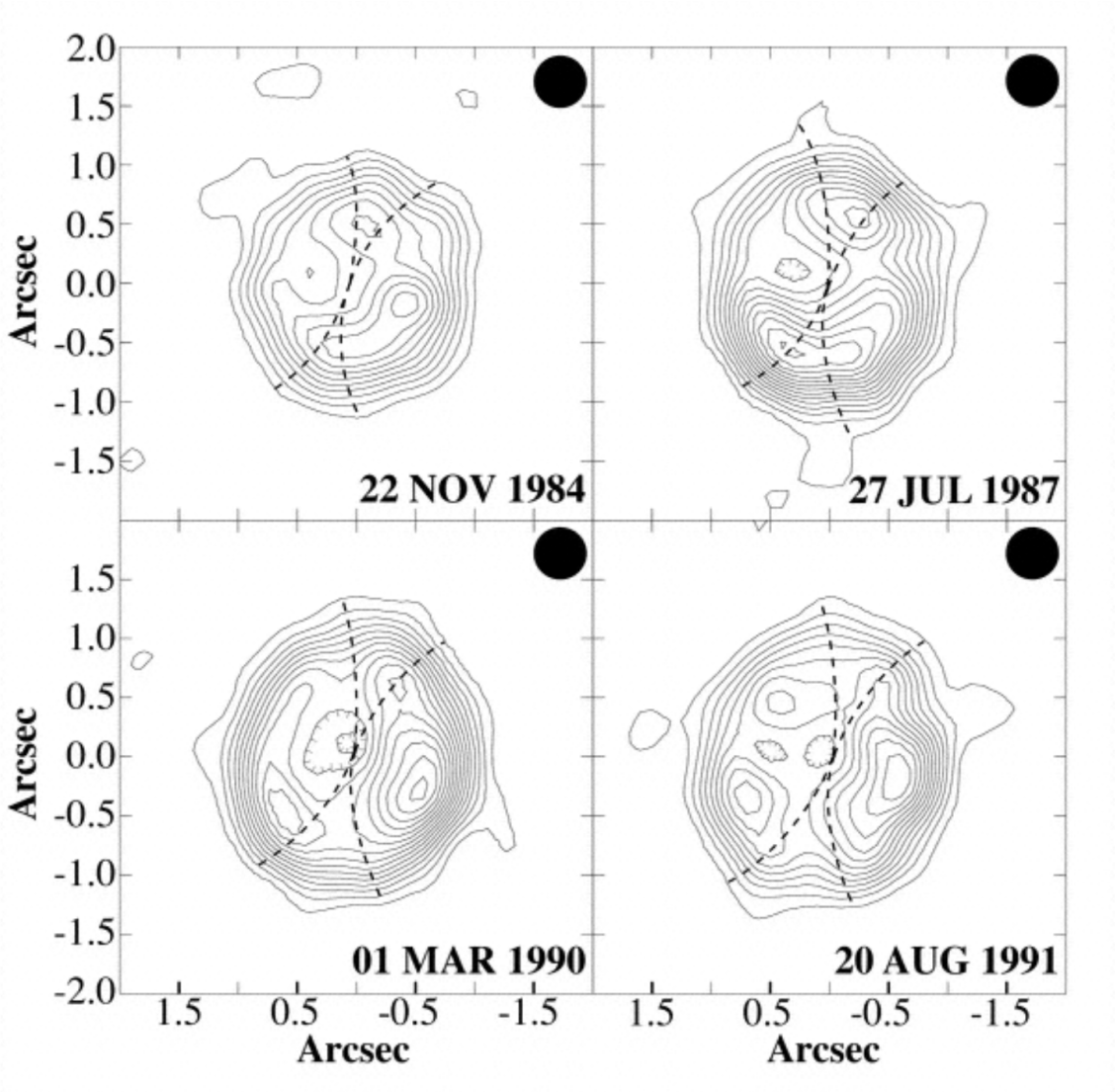

Figure 3. VLA images of Stokes I emission at $\nu = 5$ GHz of the inner thermal nebula of AG Peg. Hatched contour lines designate depressions. Black disk shows $\theta_{5\,\mathrm{GHz}} = 0\farcs45$ (570 au) at FWHM. Base contour and contour interval are $\sigma = 60\,\mu\mathrm{Jy\,beam}^{-1}$. Dashed curves convey the interaction boundary between the winds from the WD and RG, rotated about the binary orbital axis, according to a colliding wind model. Adapted from Kenny & Taylor (2007).

traits. In the resulting CWo model, the interaction zone between the two stellar winds, one from the WD and one from the RG, can become wrapped into spiral walls. Over time, the nebula could be built up from a series of spiral walls that contain interaction zone material.

The primary input parameters for Kenny & Taylor (2007)'s CWo model included distance, binary separation, and mass-loss velocities and rates of the WD and the RG. For AG Peg, all but the mass-loss rates are known from non-radio data, and mass-loss rates were estimated based on the nebula's substructure and integrated flux density. Two key inferences were identifying the interaction zone between the binary's winds (dashed curves in Figure 3) and the position angle of the binary's orbital pole (orientation of the dashed curves in Figure 3). Another important inference was the need for a range of WD mass-loss rates, with the higher rates supplementing the nebular emission along the position angle of the orbital pole.

The success of the Kenny & Taylor (2007) CWo model for AG Peg motivated theoretical and observational efforts to apply such models to the more distant S-type SySts that dominate the Galactic population (e.g., Skopal & Cariková 2015; Shagatova et al. 2016). In this sense, the inner nebula of AG Peg could be considered as being a feature that, even if not common, is at least plausibly present among the Galactic population of S-type SySts.

3.2. $D = 82$ *kpc (Draco C1)*

3.2.1. *Integrated ngVLA Detection*

If the fiducial thermal nebula is placed at Draco C1's distance, its integrated flux density (Ivison et al. 1995) falls to $S^{\rm fiducial}_{8.5\,\rm GHz} = 6.6\,{\rm mJy} \times (1.27\,{\rm kpc}/82\,{\rm kpc})^2 \sim 1.6\,\mu{\rm Jy}$.

To test for such a signal, it would suffice to conduct a search in Band 2 (Figure 2), centered at a frequency $\nu = 8\,{\rm GHz}$, with a 3σ detection threshold. This requires $\sigma^{\rm lo\,res}_{8\,\rm GHz} = 0.53\,\mu{\rm Jy\,beam^{-1}}$. An observation with an angular resolution finer than $1''$ would be desirable, as it would leverage on the XMM-Newton localization (Saeedi et al. 2019) shown in Figure 1 and also mitigate confusion from faint sources in Band 2, be they foreground, in the Draco galaxy, or background.

Using the ngVLA Exposure Calculator Tool (ngECT)[5] for the Rev. F configuration, if the Spiral+OuterCore subarray in Band 2 is tapered to a desirable low resolution $\theta^{\rm lo\,res}_{8\,\rm GHz} = 0\farcs5$ at FWHM, then the required $\sigma^{\rm lo\,res}_{8\,\rm GHz} = 0.53\,\mu{\rm Jy\,beam^{-1}}$ can be reached after an on-target time of 13 m. A detection in Band 2 could be followed up with similarly short on-target times in Bands 1 and 3 to test if $L_\nu^{\rm Draco\,C1}$ matches $L_\nu^{\rm fiducial}$ over the frequency range $\nu = 1.2 - 20.5\,{\rm GHz}$ covered by Bands 1, 2 and 3 (Figure 2).

3.2.2. *Spatially Resolved ngVLA Detection*

If the fiducial thermal nebula is placed at Draco C1's distance, its angular diameter falls to $\theta^{\rm fiducial} = 1\farcs87 \times (1.27\,{\rm kpc}/82\,{\rm kpc}) \sim 29\,{\rm mas}$.

To test for a spatially resolved nebula, suppose it is imaged in Band 2 with a desired angular resolution $\theta^{\rm hi\,res}_{8\,\rm GHz} = 7\,{\rm mas}$ at FWHM. Then the nebula encompasses $(\frac{\pi}{4} \times 29\,{\rm mas}^2)/(0.5665 \times 7\,{\rm mas}^2) = 24$ synthesized beam areas, matching the situation for Figure 3. Assuming for simplicity that the integrated flux density of Draco C1 is uniformly spread over those 24 beam areas, a 3σ detection threshold requires $\sigma^{\rm hi\,res}_{8\,\rm GHz} = 0.022\,\mu{\rm Jy\,beam^{-1}}$.

According to the ngECT for the Rev F configuration, if the full ngVLA in Band 2 is tapered to the desired $\theta^{\rm hi\,res}_{8\,\rm GHz} = 7\,{\rm mas}$ at FWHM, then the required $\sigma^{\rm hi\,res}_{8\,\rm GHz} = 0.022\,\mu{\rm Jy\,beam^{-1}}$ can be reached after an on-target time of 38 h. Data could be acquired over several scheduling blocks.

If the ngVLA observation at high angular resolution discovers a spatially resolved nebula, it could be followed up at higher sensitivity and analyzed in the ways pioneered by Kenny & Taylor (2007). A fit to a spherical shell model would yield information on the nebula's outer and inner angular diameters, electron density, and mass. A fit to a colliding wind model, augmented by non-radio data (e.g., Lewis et al. 2020), would yield information related to the interaction zone between the colliding winds, the position angle of the orbital pole of the binary, and changes in the mass loss rate from the WD.

[5] https://ngect.nrao.edu/

4. SUMMARY & CONCLUSIONS

Draco C1 is a SySt in the Draco dwarf spheroidal galaxy at a distance $D = 82 \pm 2\,{\rm kpc}$ (Kinemuchi et al. 2008). We explored whether the ngVLA could spatially resolve the continuum emission from a fiducial thermal nebula surrounding Draco C1. We found that this could be done with an on-target time of 38 h in Band 2, using the full ngVLA tapered to achieve a high angular resolution $\theta^{\rm hi\,res}_{8\,\rm GHz} = 7\,{\rm mas}$ at FWHM and an RMS noise $\sigma^{\rm hi\,res}_{8\,\rm GHz} = 0.022\,\mu{\rm Jy\,beam^{-1}}$. That this is doable at Draco C1's distance bodes well for being doable for similar thermal nebulae among the 1-50 thousand SySts estimated to reside within a Galactic radius of 10 kpc (Laversveiler et al. 2025). Discovery of a spatially resolved thermal nebula surrounding Draco C1 could be followed up to infer physical parameters of the nebula (e.g., electron density, mass) and of the SySt (e.g., interaction zone between the stellar winds, orbital pole of the binary, rate of mass loss from the WD).

ACKNOWLEDGMENTS

The National Radio Astronomy Observatory and Green Bank Observatory are facilities of the U.S. National Science Foundation operated under cooperative agreement by Associated Universities, Inc. This work was supported by awards AST-2034328 (MSIP Prototype Antenna) and AST-2334267 (ngVLA Design Activities); NRAO related activities are funded under award AST-1647378 (NRAO Operations/Development).

Facilities: VLA, JVLA, ngVLA

Software: CARTA (Comrie et al. 2021), CASA (CASA Team et al. 2022), matplotlib (Hunter 2007)

REFERENCES

Akras, S., Gonçalves, D. R., Alvarez-Candal, A., & Pereira, C. B. 2021, MNRAS, 502, 2513, doi: 10.1093/mnras/stab195

Bailer-Jones, C. A. L., Rybizki, J., Fouesneau, M., Demleitner, M., & Andrae, R. 2021, AJ, 161, 147, doi: 10.3847/1538-3881/abd806

CASA Team, Bean, B., Bhatnagar, S., et al. 2022, PASP, 134, 114501, doi: 10.1088/1538-3873/ac9642

Comrie, A., Wang, K.-S., Hsu, S.-C., et al. 2021, CARTA: The Cube Analysis and Rendering Tool for Astronomy, 2.0.0, Zenodo, doi: 10.5281/zenodo.4905459

Contreras Rojas, V., Jaque Arancibia, M., Ferreira Lopes, C. E., et al. 2026, A&A, 708, A28, doi: 10.1051/0004-6361/202556429

Corradi, R. L. M., Brandi, E., Ferrer, O. E., & Schwarz, H. E. 1999, A&A, 343, 841

Dickey, J. M., Weston, J. H. S., Sokoloski, J. L., Vrtilek, S. D., & McCollough, M. 2021, ApJ, 911, 30, doi: 10.3847/1538-4357/abe774

Ghigo, F. D., & Cohen, N. L. 1981, ApJ, 245, 988, doi: 10.1086/158875

Hjellming, R. M. 1985, in Astrophysics and Space Science Library, Vol. 116, Radio Stars, ed. R. M. Hjellming & D. M. Gibson, 97, doi: 10.1007/978-94-009-5420-5_12

Hunter, J. D. 2007, Computing in Science & Engineering, 9, 90, doi: 10.1109/MCSE.2007.55

Ivison, R. J., Seaquist, E. R., Schwarz, H. E., Hughes, D. H., & Bode, M. F. 1995, MNRAS, 273, 517, doi: 10.1093/mnras/273.2.517

Kenny, H. T., & Taylor, A. R. 2005, ApJ, 619, 527, doi: 10.1086/426309

—. 2007, ApJ, 662, 1231, doi: 10.1086/517902

Kenny, H. T., Taylor, A. R., & Seaquist, E. R. 1991, ApJ, 366, 549, doi: 10.1086/169590

Kinemuchi, K., Harris, H. C., Smith, H. A., et al. 2008, AJ, 136, 1921, doi: 10.1088/0004-6256/136/5/1921

Kuuttila, J., & Gilfanov, M. 2021, MNRAS, 507, 594, doi: 10.1093/mnras/stab2025

Lacy, M., Baum, S. A., Chandler, C. J., et al. 2020, PASP, 132, 035001, doi: 10.1088/1538-3873/ab63eb

Laversveiler, M., Gonçalves, D. R., Rocha-Pinto, H. J., & Merc, J. 2025, A&A, 698, A155, doi: 10.1051/0004-6361/202451548

Lewis, H. M., Anguiano, B., Stassun, K. G., et al. 2020, ApJL, 900, L43, doi: 10.3847/2041-8213/abb248

Meinunger, L. 1981, Information Bulletin on Variable Stars, 2016, 1

Merc, J. 2025, Galaxies, 13, 49, doi: 10.3390/galaxies13030049

Merc, J., Gális, R., & Wolf, M. 2019, Research Notes of the American Astronomical Society, 3, 28, doi: 10.3847/2515-5172/ab0429

Nussbaumer, H., & Vogel, M. 1987, A&A, 182, 51

Paczynski, B., & Zytkow, A. N. 1978, ApJ, 222, 604, doi: 10.1086/156176

Perley, R. A., & Butler, B. J. 2017, ApJS, 230, 7, doi: 10.3847/1538-4365/aa6df9

Perley, R. A., Chandler, C. J., Butler, B. J., & Wrobel, J. M. 2011, ApJL, 739, L1, doi: 10.1088/2041-8205/739/1/L1

Saeedi, S., Sasaki, M., Stelzer, B., & Ducci, L. 2019, A&A, 627, A128, doi: 10.1051/0004-6361/201834983

Seaquist, E. R., Krogulec, M., & Taylor, A. R. 1993, ApJ, 410, 260, doi: 10.1086/172742

Seaquist, E. R., & Taylor, A. R. 1990, ApJ, 349, 313, doi: 10.1086/168315

Seaquist, E. R., Taylor, A. R., & Button, S. 1984, ApJ, 284, 202, doi: 10.1086/162399

Selina, R. J., Murphy, E. J., McKinnon, M., et al. 2018, in Astronomical Society of the Pacific Conference Series, Vol. 517, Science with a Next Generation Very Large Array, ed. E. Murphy, 15, doi: 10.48550/arXiv.1810.08197

Shagatova, N., Skopal, A., & Cariková, Z. 2016, A&A, 588, A83, doi: 10.1051/0004-6361/201525645

Skopal, A., & Cariková, Z. 2015, A&A, 573, A8, doi: 10.1051/0004-6361/201424779

Skopal, A., Shugarov, S. Y., Sekeráš, M., et al. 2017, A&A, 604, A48, doi: 10.1051/0004-6361/201629593

Tandoi, C., Foster, A., Maccarone, T. J., et al. 2026, arXiv e-prints, arXiv:2605.01022, doi: 10.48550/arXiv.2605.01022

Tutukov, A. V., & Yungel'son, L. R. 1976, Astrophysics, 12, 342, doi: 10.1007/BF01003331

Washington, J. E., Lewis, H. M., Anguiano, B., et al. 2021, ApJ, 918, 19, doi: 10.3847/1538-4357/ac09ec